PNNL-38235
M3LW-25OR0404023

Light Water Reactor Sustainability Program

Radio Frequency Field Programable Gate Array Implementation of Reflectometry Cable Monitoring

S.W. Glass, J. Tedeschi, S.L. McDaid, M.S. Elen, L.S. Fifield
Pacific Northwest National Laboratory

September 2025

U.S. Department of Energy
Office of Nuclear Energy

PNNL-38235
M3LW-25OR0404023

Radio Frequency Field Programable Gate Array Implementation of Reflectometry Cable Monitoring

S.W. Glass, J. Tedeschi, S.L. McDaid, M. Elen, L.S. Fifield

Pacific Northwest National Laboratory

September 2025

Prepared by
Pacific Northwest National Laboratory
Richland, WA 99354
operated by
Battelle
for the
U.S. Department of Energy
Under Contract DE-AC05-76RL01830

SUMMARY

This document describes the development of a field programable gate array (FPGA) radio frequency system on a chip (RF SoC) adaptation and evaluation of a single-board device to perform both frequency domain reflectometry (FDR) and spread spectrum time domain reflectometry (SSTDR) for offline and online cable testing. The work builds on and leverages previous work of Pacific Northwest National Laboratory (PNNL) on airport millimeter wave technology by using the same development hardware employed in that program. The current work is performed under sponsorship from the U.S. Department of Energy (DOE) Light Water Reactor Sustainability (LWRS) program Materials Research Pathway. The task objective is to confirm and demonstrate feasibility to adapt FPGA technology for a cost-effective multiplexed single-board electronic module to perform cable tests that are equivalent to commercial and laboratory test instruments for FDR and SSTDR cable tests. The developed two-channel (extendable to seven channels) system was compared to dedicated and proven test instruments and shown to produce equivalent results on a range of cables and with a range of damage types. The FPGA reflectometry test board is one of several technologies that could facilitate implementation of online monitoring of safety-critical cable systems. Other required tools include:

- Coupling technology (inductive or capacitive) that can protect the test instruments from damage from high voltage levels in energized cables (up to 2000 VAC for low voltage systems and 15 kV for medium voltage nuclear power plant applications).
- Automatic measurement analysis to recognize cable damage and degradation. Note that reflectometry signals are complex and not well suited for simple threshold alarms. Advanced signal processing approaches like baseline reference signal subtraction and machine learning based on a library of training data will be enabling for practical applications.

PNNL and others have investigated and are continuing development to make these kinds of tools available for a complete online monitoring system.

The FPGA system architecture, including hardware description and an outline of the software, are described within this report. The complete copyright-protected software is provided in an appendix such that one skilled in FPGA development could replicate the developed system.

ACKNOWLEDGEMENTS

This work was sponsored by the U.S. Department of Energy, Office of Nuclear Energy, for the Light Water Reactor Sustainability (LWRS) program Materials Research Pathway. The authors extend their appreciation to Pathway Lead Dr. Xiang (Frank) Chen for LWRS programmatic support. This work was performed at the Pacific Northwest National Laboratory (PNNL). PNNL is operated by Battelle for the U.S. Department of Energy under contract DE-AC05-76RL01830.

CONTENTS

FIGURES

ACRONYMS

AC	alternating current (60 Hz in the US)
ADC	analog-to-digital converter
AMD	Advanced Micro Devices
CUT	cable or cable segment under test
DAC	digital-to-analog converter
DC	direct current
DMA	Direct Memory Access
DOE	U.S. Department of Energy
EMI	electromagnetic interference
EQ	environmentally qualified
FDR	frequency domain reflectometry
FFT	fast Fourier transform
FPGA	field programmable gate array
Hz	Hertz (per second, unit of frequency)
IF	intermediate frequency
I/O	input/output
LWRS	Light Water Reactor Sustainability
LOCA	Loss Of Coolant Accident
NPP	nuclear power plant
PCB	printed circuit board
PN	pseudo-random noise
PNNL	Pacific Northwest National Laboratory
RAM	random access memory
RF	radio frequency (typically 3 kHz to 300 GHz)
RF SoC	radio frequency system on a chip
SSTDR	spread spectrum time domain reflectometry
SMA	Sub-Miniature Version A connector
SNR	signal-to-noise ratio
V	volt
VNA	vector network analyzer

1. INTRODUCTION

Nuclear power plant (NPP) electrical cables in the U.S. were initially considered passive components with service lifetimes equivalent to the 40-year operating life of the plant. Most U.S. plants have applied for or already received a renewal of their original 40-year license, and several plants have received a subsequent license renewal to operate up to 80 years. Operating experience has shown that, while cable failures are infrequent, cable performance degradation can occur over time due to several factors including heat, moisture, chemical exposure, radiation, flexure, abrasion, and pinching, as well as connector and splice crimp workmanship issues. These aging factors can lead to insulation materials crumbling, separating, eroding, and experiencing diminished dielectric properties. It is understood that insulation cracking and subsequent exposure of conductors could lead to low-resistance, short or open circuits and corresponding circuit failures with associated safety risks and/or operational outages. Due to these considerations, plant operating license renewal requirement implementation of a cable aging management plan that maintains an inventory of cables in adverse local plant environments and involves a testing plan for cables at risk of degradation due to aging. Condition monitoring is used to determine if aging equipment is suitable for continued service (NRC 2010). Cable testing typically involves:

- Scheduling the cable test during an outage or period where the critical systems can be taken out of service.
- Disconnecting the cable.
- Performing one or more tests of the cable from one or both ends of the cable. (Note that cables are commonly buried in conduit or otherwise inaccessible for most of their length).
- Typically, tests conclude that the cable is good, bad, or needs further evaluation. Practical management of a “bad” or “needs further evaluation” cable may include full replacement or identification of damage location and splicing in of a new piece of cable then re-testing.
- Once the cable segment tests “good”, the cable must be re-connected and the system returned to service. Reconnections are performed by trained staff but experience shows that workmanship errors are among the most common causes of cable failure (Pyy 2001).

This periodic testing procedure can be difficult to schedule during plant outages and around other operational concerns; is disruptive in that it involves taking circuits offline; is labor-intensive for cable disconnection, testing and reconnection; and can itself introduce cable issues in the process of manual handling of aged cables.

An attractive alternative to the current testing process would be online testing of cables without having to power them down or disconnect them. Online cable test technology and experience for nuclear power plants is limited (Glass, Fifield, and Bowler 2020). Partial discharge testing may be used on critical systems but is most applied to service critical medium and high voltage transmission and distribution lines (Ahmed and Srinivas 1998, Han et al. 2023). Commercial online reflectometry systems have been widely applied to low voltage aircraft and electric rail systems but have not been broadly used in NPPs (Glass, Fifield, and Bowler 2020). Fiber optic systems are used for both onshore and offshore high voltage distribution lines but are rarely found on the low or medium voltage systems typical of NPPs.

The present research is primarily focused on low and medium voltage reflectometry test techniques that may be developed into NPP online monitoring systems. However, the technology developed may have significantly broader potential for other critical cable monitoring. Reflectometry tests generally consist of injecting a high frequency signal onto the conductor that propagates equally in both directions along the cable at a velocity characteristic of the cable. If the wave encounters an impedance change (due to conductor or insulation damage), a portion of the wave energy is reflected toward the injection point. The test instrument monitors for reflected signals and if a signal is detected, the location of the impedance

mismatch and corresponding damage can be estimated using the known velocity of propagation and time delay. The high frequency interrogation signal can be a simple pulse, but a simple pulse produces a notoriously noisy signal that can be difficult to interpret. Noise in the reflectometry data can be mitigated by injecting either a swept frequency chirp (for frequency domain reflectometry) or a spread-spectrum pseudo noise (PN) chirp for spread spectrum time domain reflectometry.

Essential required tools for a reflectometry-based online monitoring system for low and medium voltage NPP cables include:

- A rugged instrument with analog-to-digital inputs, digital-to-analog outputs, and onboard computational capability to produce a noise-tolerant processed reflectometry signal. Preferably this instrument would have the capability to connect to multiple cable systems thereby reducing per-asset test costs. Development and adaptation of the field programmable array (FPGA) radio frequency system on a chip (RF SoC) system addresses this need and is the primary subject of this report.
- Coupling technology (inductive or capacitive) that can protect test instruments from damaging high voltage levels (up to 2000 VAC for low voltage systems and 15 kV for medium voltage nuclear power plant applications). Pacific Northwest National Laboratory (PNNL) has demonstrated a clamshell inductive coupler that meets this need (Glass et al. 2025) and will be briefly described.
- Automatic measurement analysis to recognize cable damage and degradation. Note that reflectometry signals are complex and not well suited for simple threshold alarms. Advanced signal processing approaches like baseline reference signal subtraction and machine learning based on a library of training data (Glass et al. 2024) will also be briefly described.

PNNL and others are continuing development to make these kinds of tools available for a complete online monitoring system. Each of these tools will be briefly described, but the focus of this report will be the development of hardware and software for the reflectometry instrument. The tools are becoming available and can be used to support advanced condition monitoring of cables in plant extended operation. Effective online monitoring of cable health might even be used one day to maintain the qualification status of safety related cables based on their verified condition rather than relying on their time-based qualified life.

1.1 FREQUENCY DOMAIN REFLECTOMETRY

Frequency domain reflectometry (FDR) is being used in NPPs, particularly to isolate locations of concern on de-energized cables. The FDR instrument, typically based on a vector network analyzer (VNA), is connected to two conductors in the cable assembly, one considered the primary conductor under test and the other considered the system ground, as shown in Figure 1. This interface typically produces a reflection from the connection of the FDR lead wire to the cable under test. The FDR instrument directs a swept frequency chirp onto a conductor and then listens for reflections from impedance changes along the cable length or to a parallel conductor within the cable bundle (Glass et al. 2017). Significant noise immunity and sensitivity to subtle impedance changes can be achieved by detecting reflections in the frequency domain, filtering, and converting the frequency domain data to the time domain with an inverse Fourier transformation. The signal may then be converted to the distance data using the velocity of propagation characteristic of the cable. The bandwidth for FDR is software adjustable, but experience shows the best responses for frequency values from 50 MHz to 500 MHz. Higher bandwidth FDR signals produce sharper peaks capable of spatially resolving more closely spaced impedance changes. Higher frequencies, however, do not propagate as far along a cable length due to signal attenuation. Testing is performed at multiple bandwidths, providing analysts with both high- and low-frequency data to consider in dispositioning test results. FDR instruments are generally restricted to relatively low voltage input and cannot tolerate testing on energized cable systems.

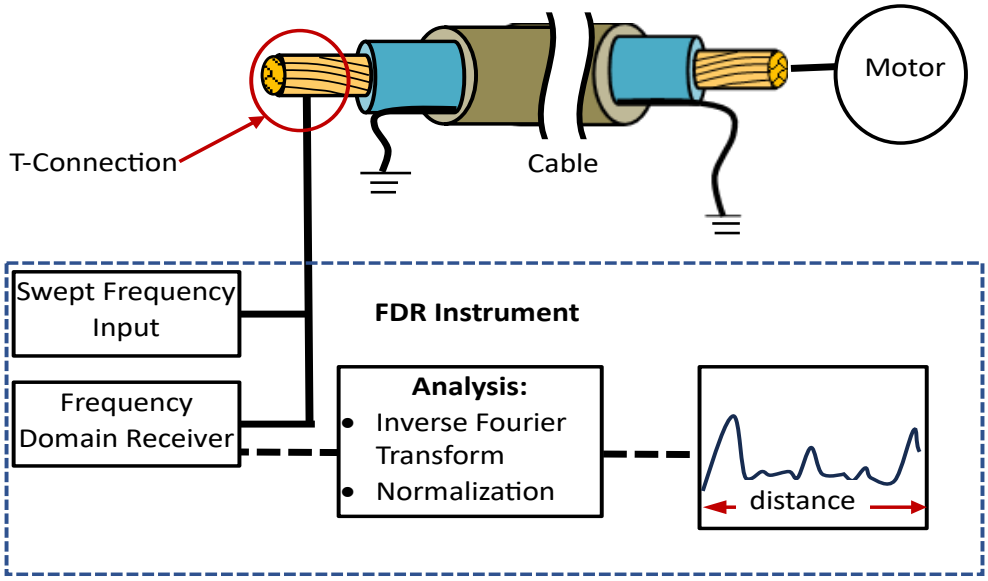

Figure 1. The FDR cable test introduces a swept frequency chirp onto a conductor and then monitors reflections from impedance changes along the cable length.

One exception to this is the commercial technology of the Wirescan company of Norway (wirescan.no) who recently claimed the ability to couple to energized lines up to 33 kV (Wirescan 2022). This coupling connects to the primary conductor via a "T" connection with both capacitive and inductive pickups. Details of this design are proprietary to Wirescan.

1.2 SPREAD SPECTRUM TIME DOMAIN REFLECTOMETRY

Spread spectrum time domain reflectometry (SSTDR) produces a similar plot to FDR, but all processing is in the time domain (Furse 2006). A pseudo-random noise (PN) code modulated with a square wave carrier through a high-pass filter is input onto the cable conductor via a "T" connection that allows testing of the cable online. The instrument monitors for any reflected response from cable anomalies (see Figure 2). The SSTDR processes the signal by performing a cross-correlation, comparing the input PN code to any reflected signal detected. The cross-correlation algorithm produces a robust noise-tolerant signal response like FDR, essentially using a matched filter approach. The effective bandwidth vs. modulation bandwidth is different for FDR than it is for SSTDR. Where FDR utilizes a frequency-modulated continuous wave chirp, sweeping over a bandwidth with very sharp edges at the start/stop of the chirp, SSTDR modulates a carrier with a specific modulation frequency equating to half of the 3 dB bandwidth (e.g., 20 MHz modulation equates to ~40 MHz of bandwidth). However, there are subtleties in the SSTDR bandwidth definition as the edges are not sharp start/stop points as in the FDR case; they gradually roll off with SSTDR and thus create a wider effective bandwidth that can be used for fine time-domain resolution. With these differences, generalizations about lower vs. higher bandwidth still apply.

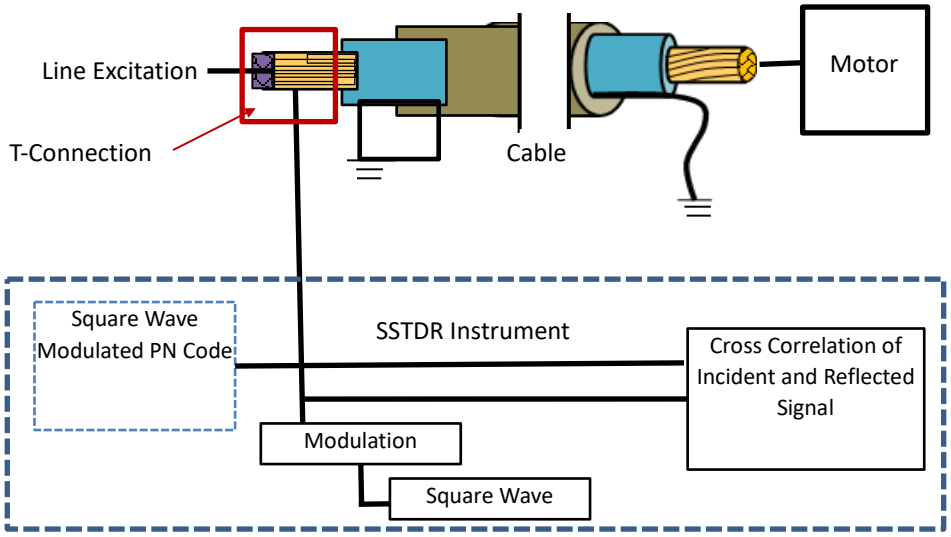

Figure 2. SSTDR cable test applies a PN code to the conductor for cross-correlation analysis.

Currently, SSTDR is offered commercially through LiveWire Innovation. One distinct advantage of the LiveWire SSTDR is that the circuitry can be used for measurements on energized cable up to 1 kV. The LiveWire instrument, however, is hardware-limited to frequency bandwidths of 48 MHz. To permit higher bandwidths to be examined, a custom, laboratory-grade SSTDR was implemented using an arbitrary waveform generator to create spread spectrum waveforms and a digitizing oscilloscope to capture the reference and return signals (Glass et al. 2023). The digitized signals were then processed in Python-based implementations of a cross-correlation function with custom frequency domain windowing. This laboratory instrument SSTDR extended available bandwidth up to 500 MHz, although actual cable test data were quite noisy and therefore not useful for manual visual analysis for bandwidths above 200 MHz on 100 ft cables. The higher frequencies however do contribute substantially to machine learning reflectometry automated damage detection (Glass et al. 2024).

1.3 INDUCTIVE CURRENT COUPLER

The laboratory instrument SSTDR, VNA FDR, and most other RF instruments have an input limit of 10 to 30 V at 60 Hz or with direct current (DC) exposure. Without a protection/isolation circuit, high-voltage DC or 60 Hz alternating current (AC) voltage (typically from 120 V to 15 kV) will damage costly RF test equipment. An ideal way to perform these measurements is with a high-pass filter that can suppress DC and 60 Hz low-frequency power voltages and allow higher RF signals to pass through. However, due to manufacturing constraints for high voltage components, parasitic inductance, resistance, and capacitance are present making the high voltage components only suitable for lower frequency operation, typically lower than 10 MHz. Therefore, instead of a classical filter, a current probe that supports reciprocal measurements is used in this work. The commercial current probe can both transmit and receive. It can also be used to inject and sense RF signals on a live voltage line while providing low-frequency isolation to RF test equipment.

RF current probes are based on AC behavior described by Ampere-Maxwell equations. In the application of a current probe (see Figure 3), an alternating current along the primary conductor, I_P, will induce a magnetic flux, B, within the core of the ferromagnetic material surrounding the primary conductor. A readout conductor is wrapped around the ferrite core to measure a secondary current, I_S, that is proportional to the number of turns around the ferromagnetic core, N, in relation to the primary current. The architecture shown in Figure 3 is used for commercial applications measuring current on AC lines for single conductors as shown in Figure 4 (Fluke 2022). The design of the core and number of windings

influence the characteristic impendence and set the current at which the ferrite core itself will saturate. Specific design considerations also include elements such as parasitic capacitance between secondary windings for high-frequency current probes. RF current probes are transformers that measure or produce a voltage in a 50-ohm load proportional to the current flowing through the probe inner diameter based on the characteristic impedance of the probe. This is referred to as the transfer impedance of the probe and leads to the insertion loss through the probe vs. frequency (Yao, Ma, and Yu 2014) expressed as:

$$IL = 20 \log_{10}(R) - Z_T, \qquad \text{Eq. 1}$$

where IL = insertion loss (dB), R = impedance of the RF circuit = 50 ohms, and Z_T = transfer impedance (dB ohms). The insertion loss values through RF probes are in the -40 to -80 dB range for 60 Hz signals, while values in the MHz frequency range are typically less than -10 dB. This creates a non-contact, frequency-selective probe through which RF signals can interact with live voltage lines.

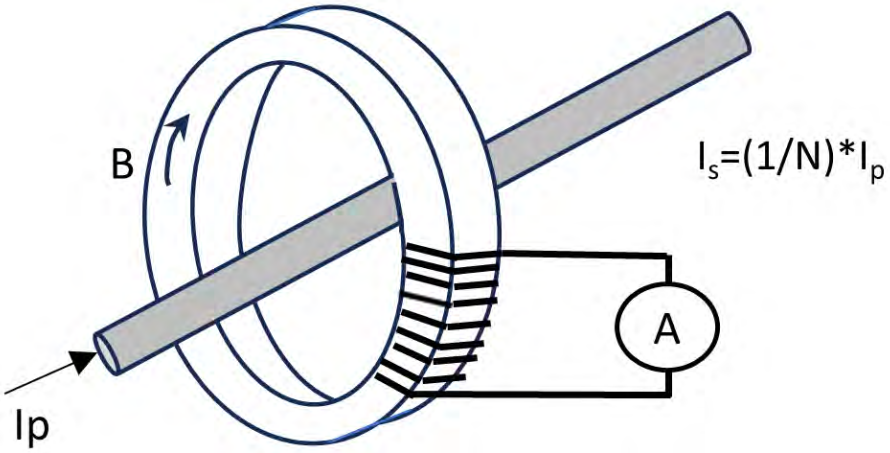

Figure 3. Architecture of a typical current probe.

Figure 4. Example of a commercial clamp-on current probe.

A standard application for commercial RF current probes is the sensing and investigation of the presence of electromagnetic interference (EMI) on conductors typically manifesting as stray signals that have coupled onto the lines. Another is the induction of EMI onto a line to determine the sensitivity of a circuit to external EMI. The use case of the RF current probe in this work is for both transmission and reception of RF signals to perform reflectometry measurements while maintaining both physical and frequency isolation far from the high DC or 60 Hz AC voltage. An A.H. Systems injection current probe ICP-622 (A.H. Systems 2023) was selected (see Figure 5) to provide an operational RF bandwidth from 1–500 MHz and high isolation from DC and 60 Hz as seen in the insertion loss of the probe in Figure 5. Initial tests with the clamshell coupler revealed a response sensitivity to the conductor being centered and fixed within the coil. A three-dimensional printed plastic centering assembly and absorber shielding layer were added to the commercial unit to minimize this issue.

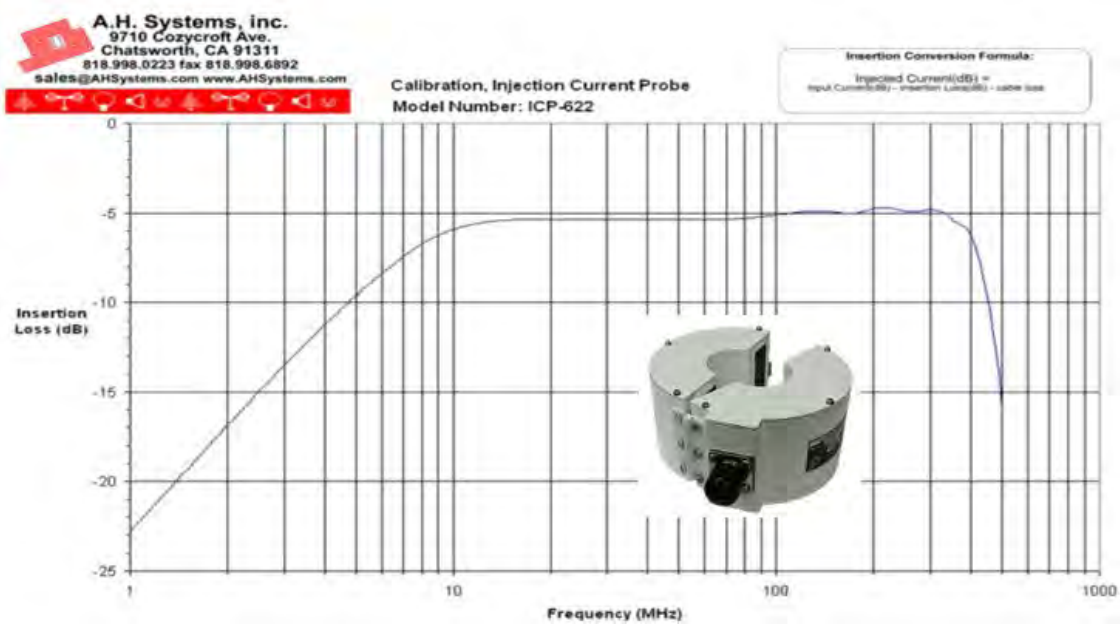

Figure 5. This product provides good response from 1 to 500 MHz with low frequency isolation including operational line frequencies.

2. FIELD PROGRAMABLE GATE ARRAYS

FPGAs have revolutionized electronic development technology by offering a versatile platform for implementing complex digital designs. Their reconfigurability and ability to handle high-speed data processing make them ideal for applications such as cable reflectometry tests that require:

- A digital-to-analog converter (DAC) to produce the reflectometry excitation waveform
- An analog-to-digital converter (ADC) that will capture and store the output and reflected signals associated with the reflectometry test.
- A multi-channel multiplexer to allow coincident or sequential processing of signals to and from multiple cables using a single card.
- A programable computational unit that will produce the output waveform and process the input waveform using time-based correlation algorithms, frequency domain capture and transform algorithms, and inverse frequency domain transforms to return signals to a time/distance display.

FPGA development kits have a rich library of examples to aid with specific development applications. The cable test focus of this project bears similarity to prior work performed by PNNL for millimeter-wave airport security applications.

3. DEVELOPMENT OF AN FPGA MULTI-CHANNEL FDR AND SSTDR DEVICE

PNNL selected an RF SoC developed by Xilinx, part of Advanced Micro Devices (AMD). The RF SoC ZCU111 provides a multi-channel high speed DAC and ADC configuration, which enables high-frequency transmission and reception with digitally synthesized waveforms. The benefit of the digitally created waveforms is the flexibility and adaptability of waveforms in terms of power, frequency, duration, and modulation.

3.1 HARDWARE ARCHITECTURE

The high-level system block diagram for cable measurements utilizing the RF SoC ZCU111 is shown in Figure 6. A host computer uploads test waveforms to the ZCU111 via a local network connection; the waveforms are transferred into memory on the ZCU111 and uploaded to the DACs. These are then transmitted as a voltage vs. time waveform from the ZCU111 into the RF front end which amplifies, filters, and transmits the waveform. The output of the RF front end provides a standard Sub-Miniature Version A connector (SMA) connector head where the RF system is calibrated (0 dB amplitude and 0-degree phase). The SMA is connected to the cable under test using direct connection methods or indirect methods such as the RF current probe previously discussed. As waveforms interact with the cable under test (CUT) and are reflected to the measurement system, the RF front end amplifies the signals and sends them to the ZCU111 ADCs for digitization. These digitized waveforms are stored in memory onboard the ZCU111 and transferred to the host computer for processing. All waveform creation and processing currently take place onboard the host computer for flexibility and practicality. Note that this strategy enables both FDR and SSTDR measurements in a matter of seconds for continuously monitoring systems as compared to a manual test program that may support repeat tests only every 2 to 6 years or more. Additional development could decrease the time required to take measurements by implementing these processes onboard the FPGA.

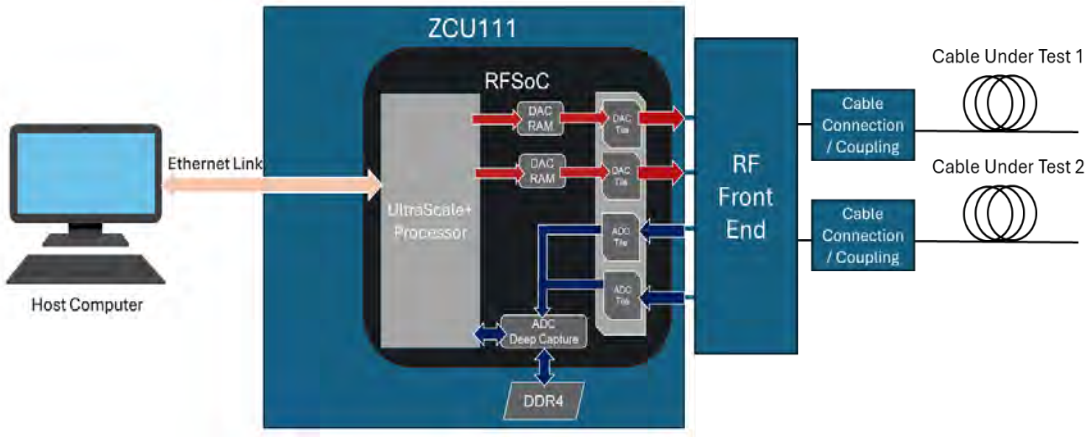

Figure 6. RF SoC high level architecture shown with RF Front End and Cable(s) Under Test.

Figure 7 shows a photograph of the RF SoC installed in a 2U rack with the RF front end installed. It is worth noting that additional hardware development could enable the RF SoC to be integrated with the RF front end onto a single printed circuit board (PCB) along with all required power supplies into a form factor similar in size to the Copper Mountain vector network analyzer (VNA).

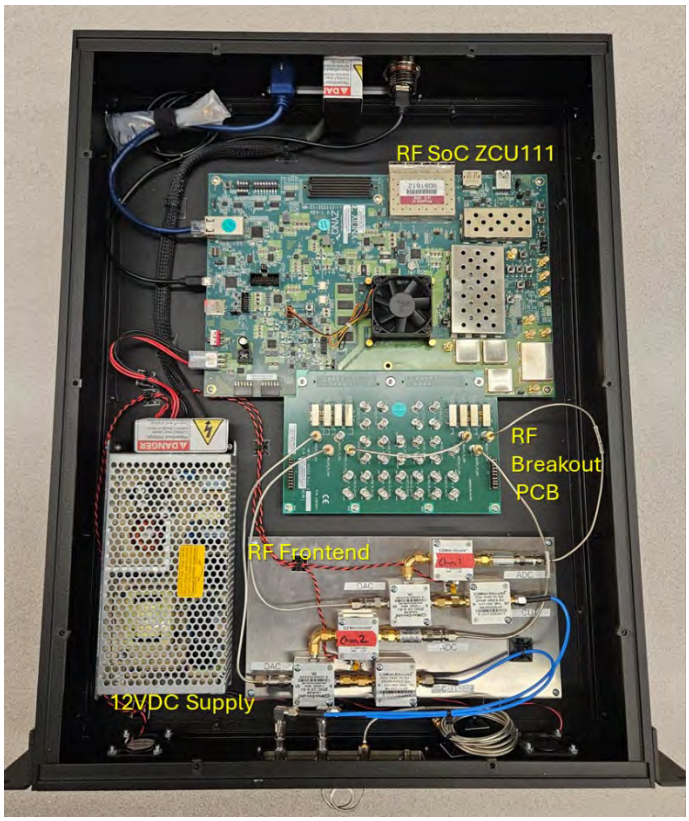

Figure 7. PNNL RF SoC hardware configuration.

The RF front end that interfaces with the ZCU111 (Figure 8) is designed to provide amplification, filtering, and impedance matching for the broadband waveforms, digital system, and CUT. In the current configuration, the evaluation PCB from Xilinx has mediocre impedance matching from its DAC and ADC channels, therefore 6dB RF attenuators were used to prevent multi-path signal reflections taking place between the digital and RF system. Additionally, it was determined that the image frequencies that alias about the RF SoC sample rate of 2 GHz, presented strong artifacts and required low pass filtering on the receive input, thus PNNL installed a coaxial low pass filter to suppress the undesired image frequencies.

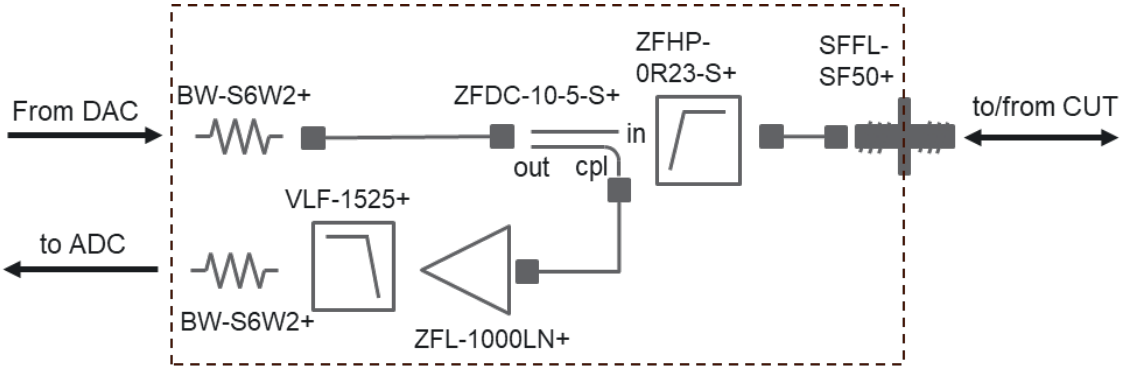

Figure 8. High-level schematic of a single RF front end channel.

3.2 SOFTWARE ARCHITECTURE

Practical implementation of a cable reflectometry monitoring system requires both acquisition and analysis level software. The analysis level software treats the acquired reflectometry data to estimate the cable condition and to monitor for any significant change that may require operator action. Reflectometry data is notoriously noisy and does not support a simple threshold alarm monitoring strategy. Under a separate program however, PNNL and others have shown machine learning (ML) approaches can be successful at identifying early cable faults (Glass et al. 2024). The ML code is typically written in Python and employs various strategies to train a model to recognize signal changes indicative of damage and alert the operators to consider action before the cable fails. The ML aspect of the monitoring system relies on the acquisition software and hardware.

The acquisition software for the FPGA hardware is broken into 3 primary components:

1) High-level user interface software scripts
2) Signal processing for all measurement modalities
3) FPGA configuration for interconnections, input/output (I/O) and logic.

The high-level user interface scripts are built using Python. A user inputs a test matrix that has been configured previously in Microsoft Excel. The test matrix includes information for all measurements including cable types / descriptions and configurations for the FDR/SSTDR bandwidths. The high-level script imports this test matrix and, from a user selected start index, sequentially progresses through the test matrix measurements with feedback to the user. The high-level script automatically communicates with the FPGA, uploading appropriate waveforms for the given measurement, saving and processing data, and creating folders on a shared drive to place the resulting measurements of both raw and processed data.

The signal processing scripts developed for this effort leverage previous developments of SSTDR and FDR processing (Glass et al. 2023). Unique to the updated configuration, the SSTDR processing employs a calibration to the reference waveform. It is computed from an open circuit measurement at the RF connector that interfaces with the CUT and subtracted by a coaxial short circuit placed at the same location. This performs two key features: 1) the reference waveform time shift and frequency structure is now referenced through the entire RF front end chain such that 0 time is now at the CUT RF connection similar to the FDR data sets, and 2) the Open and Short data sets from the primary reflection are 180 degrees out of phase, such that the subtraction boosts their amplitude, and removes signal leakage through the ZFDC-10-5-S+ coupler that would fold into the data. Additional details on cross correlation, frequency domain windowing and sampling are included in Appendix 1.

For the FDR system, classical 1-port VNA calibrations (Copper Mountain 2020) were employed using Open, Short and 50-ohm coaxial terminations. These three measurements provide error corrections for amplitude and phase, integrating the RF SoC and RF front end into the system calibrations placing 0-degree phase and 0 dB magnitude at the CUT interface point, thus any changes are due to the system under test and not the measurement system itself. FDR calibration and processing details are outlined in Appendix 1.

The FGPA architecture was developed such that custom generated waveforms can be loaded into Block RAM of the FPGA and output through the DAC, while simultaneously capturing synchronized data on an ADC into a Direct Memory Access (DMA) channel. The FPGA implementation incorporates the Xilinx IP RF Data Converter, which enables the main feature of the RF SoC, direct RF sampling. This Block provides the critical interface between the digital signal processing domain and the RF analog front end, handling the high-speed sampling requirements necessary for both SSTDR and FDR measurements.

The supporting architecture consists of several key components: waveform storage in dedicated Block RAM modules for high-speed access, synchronized timing control to ensure precise ADC/DAC coordination and DMA channels for efficient data transfer to the host system.

A custom software program was developed to initiate the measurement sequence by triggering the output of the stored custom waveforms through the DAC while simultaneously capturing the corresponding response waveform from the ADC. The captured data is then transferred through the DMA interface and output to files accessible by the host computer for signal processing and analysis. This architecture provides flexibility to support various waveform types and measurement configurations.

4. TEST AND EVALUATION

Testing and evaluation of the RF SoC SSTDR/FDR system was broken down into multiple stages: 1) calibration validation, 2) performance comparison to current standards, and 3) extrapolated performance evaluation with multiple conductors.

The calibration methods used with the RF SoC system were first confirmed by utilizing the same calibration technique on a Copper Mountain VNA in a post-data collection evaluation and comparing the results to a standard VNA 1-port calibration. Figure 9 below shows the test configuration for a standard VNA 1-port calibration vs. the 2-port calibration that is treated as a 1-port via a directional coupler connecting the VNA ports 1 and 2.

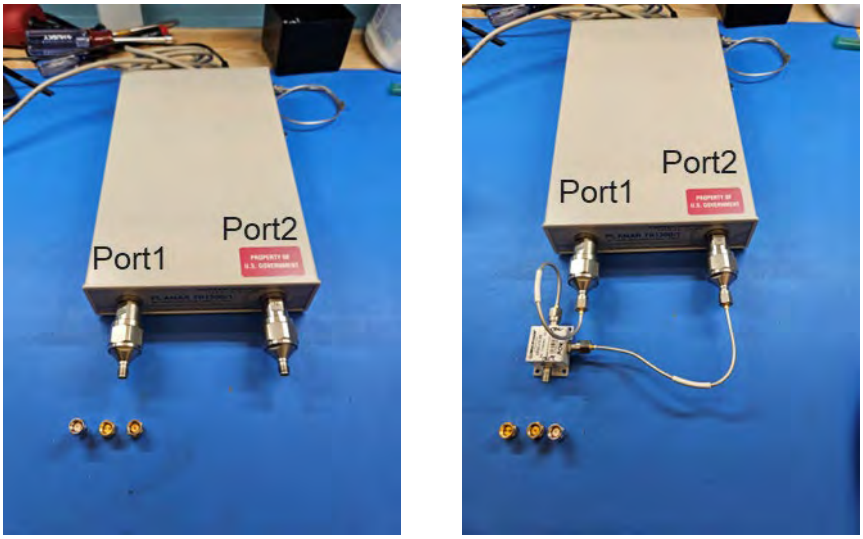

Figure 9. Copper Mountain VNA with std 1-port connect (left), and 2-port test configuration (right) with RF Open/Short/Load calibration standards in lower left of images.

VNA calibration utilizes Open/Short/Load RF coaxial standards. For the 1-port case, these standards are measured only on Port 1 with internal signal paths enabling transmission and reception from a single port, and corrections applied to Port 1. For the 2-port test configuration, an external directional coupler is used to connect ports 1 and 2, treating port 1 like the transmitting DAC port from the RF SoC, and port 2 like the receiving ADC on the RF SoC, and the 3-port direction coupler connects these ports to the cable under test (Figure 10). To confirm the accuracy of the 2-port calibration method, the same test cable was measured in both configurations with their respective calibrations applied and results compared.

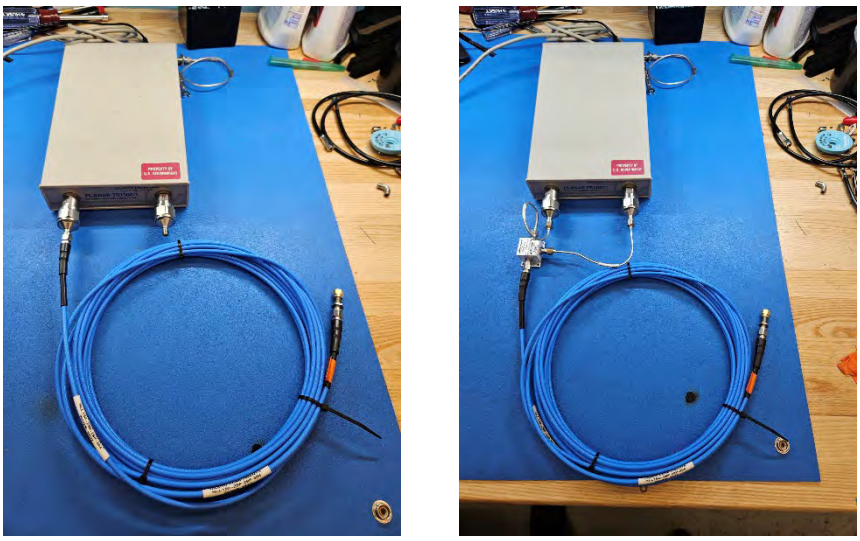

Figure 10. RF test cable measured on standard 1-port VNA configuration and 2-port VNA configuration to validate the calibration method that would be utilized with the RF SoC.

The magnitude and phase corrections created by the calibration standard measurements were applied to the shorted cable under test. The results show a direct overlay between the standard 1-port calibration and the manual 2-port calibration method demonstrating that approach and manual calibration calculations provide an accurate means for calibrating the RF SoC (Figure 11).

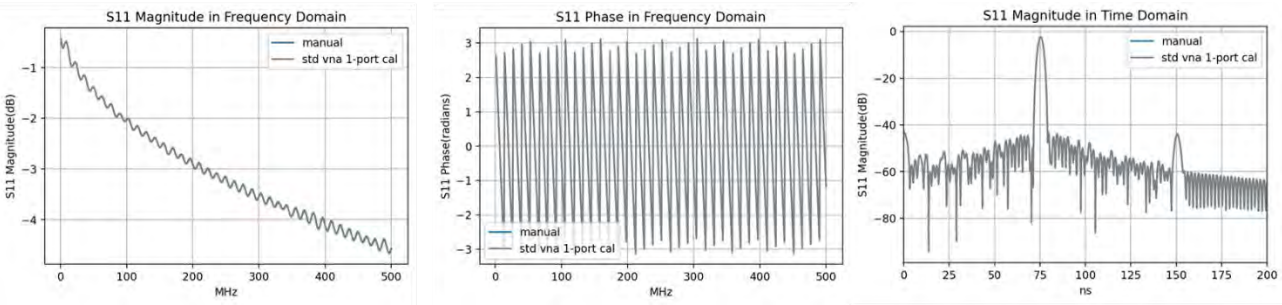

Figure 11. Shorted RF test cable comparison plots between std 1-port calibration and manual 2-port calibration.

To test the RF SoC and its calibrated response, the RF front end previously discussed and shown in Figure 8 was installed outside the RF SoC, connecting its ADC and DAC channels to their respective ports. For comparison, a separate measurement was made with the Copper Mountain VNA connected with port 1 to the RF front end DAC input, and VNA port 2 connected to where the ADC channel would go. This provided the ability to do a full manual calibration of the VNA with the RF front end, calibrate the RF SoC, and compare the test results for the shorted RF cable (Figure 12).

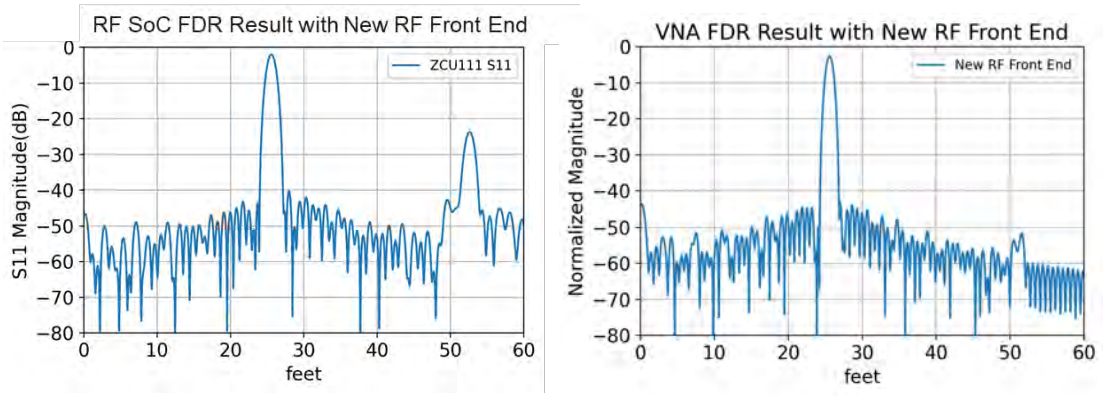

Figure 12. FDR performance comparison between RF SoC (left), and Copper Mountain VNA (right).

The resulting waveforms produced comparable amplitudes, signal-to-noise ratio (SNR), and location of the detected short. However, the RF SoC result did produce a stronger secondary multi-path reflection as shown at approximately 53 ft. There are two contributing factors here for the secondary peak of the RF SoC. The first is the overall impedance match of the RF SoC DAC transmit chain. This could be overcome in future designs by utilizing well-matched RF amplifiers followed by attenuators to create minimal gain on the transmit side. The second is high isolation from the DAC output to the cable under test. Additionally, harmonics generated in the ADC, DAC and front end can produce peaks that, due to being two times the frequency, result in a secondary peak at two times the range. These effects can further be reduced by increased filtering, LNA linearity and by optimizing ADC input voltages. The overall results show good agreement between the RF SoC and the VNA, with potential for future improvements.

For SSTDR, the updated processing includes an initial calibration that is collected as part of the FDR calibration. For this case, calibrating the SSTDR reviewed different waveforms that could be used for the reference waveform in the cross correlation calculation, recall that the reference waveform is compared against the time shifted data from the cable under test, where the resulting correlation peaks are due to the relative time shifts between the reference waveform and the measured response from the cable under test. Three reference waveforms were used to compare the resulting correlation response from the shorted RF test cable: 1) ideal SSTDR waveform (input to DAC), 2) measured SSTDR waveform from a RF Short standard, and 3) difference between measured SSTDR waveform from RF open and short calibration standards. Note that the calibration standards were placed directly at the output of the RF SoC RF front end and measured during the same calibration process as the FDR/VNA mode.

Correlation results for the three different reference waveforms applied to the same SSTDR measurement in post processing show interesting results (Figure 13). In the ideal standard waveform case, it produces a clean response but with a time shifted result that would need to be manually corrected. In the case where the short standard is used, since it propagates through the entire DAC/RF front end/ADC and undergoes the same baseline time shifts that a true measurement would undergo, it appropriately shifts the resulting waveform to the appropriate distance. Finally, in the case with a Short–Open standard used for the reference waveform, since the reflections off the Open and Short are 180 degrees out of phase, the subtraction causes them to add, but there are non-ideal signal leakage effects in the directional coupler that do not undergo the 180 degrees phase shift from the calibration standards, and as such, these are common to both measurements and cancel out in the subtraction process. One can observe this impact by the range domain ‘noise’ floor of the Short–Open case having less structure due to the removal of the non-ideal coupled path.

The testing results of the SSTDR reference waveform determined that the Short–Open standards produce the best results and was adopted into the SSTDR signal processing scripts.

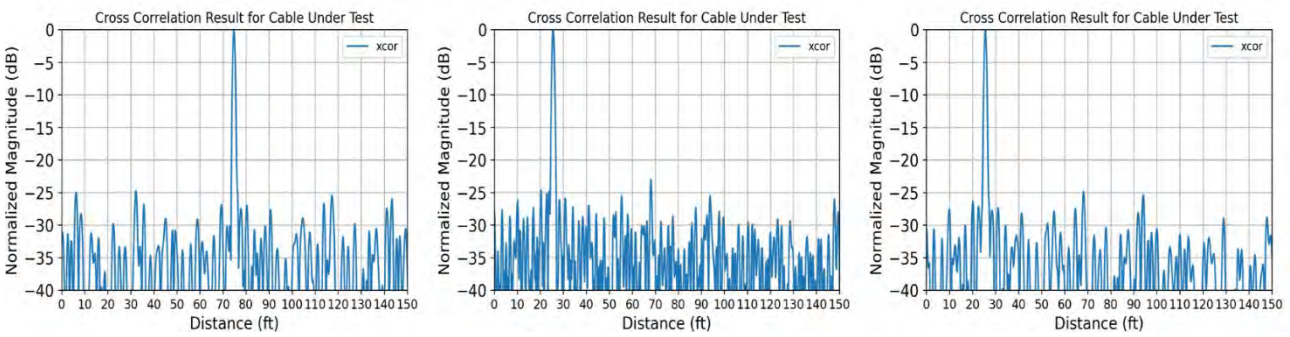

Figure 13. Shorted RF test cable SSTDR correlation results for different reference waveforms. Ideal SSTDR waveform (left), Short standard waveform (middle), and Short–Open standard (left).

5. TEST RESULTS

The RF SoC system was tested in several configurations to: 1) investigate advantages of the multi-channel capabilities provided by the RF SoC, and 2) confirm good performance in comparison to the existing commercial and laboratory reflectometry systems.

The RF SoC system is configured to have two channels operating simultaneously as it steps through the FDR and SSTDR measurements. This is designed to provide the ability to monitor multiple cables or conductor pairs simultaneously and review performance between them.

The test configuration below (Figure 14) was used to measure channel 1 vs. channel 2 measurements of the same cable. A low voltage, approximately 170 ft long three conductor shielded cable was used, where the blue and red conductors were shorted at the cable end, and the black conductor left open circuit. The blue and red conductors were connected to the + and – terminals respectively in a BNC adapter. This connection was first placed on the RF SoC system and measured on channel 1, then moved to channel 2 and collected (Figure 15). The results comparing the performance between channel 1 and channel 2 of the RF SoC system showed excellent agreement. Figure 15 shows the results for the two separate channels measuring the same shorted ~170 ft low voltage cable with excellent agreement even out to the extended range of the cable end.

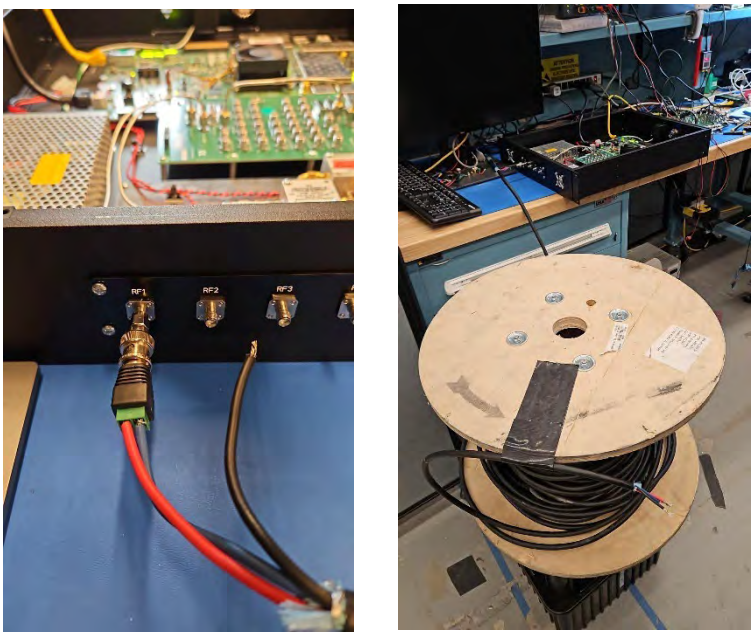

Figure 14. CUT connection to the RF SoC system channel 1 (left), CUT test configuration (right).

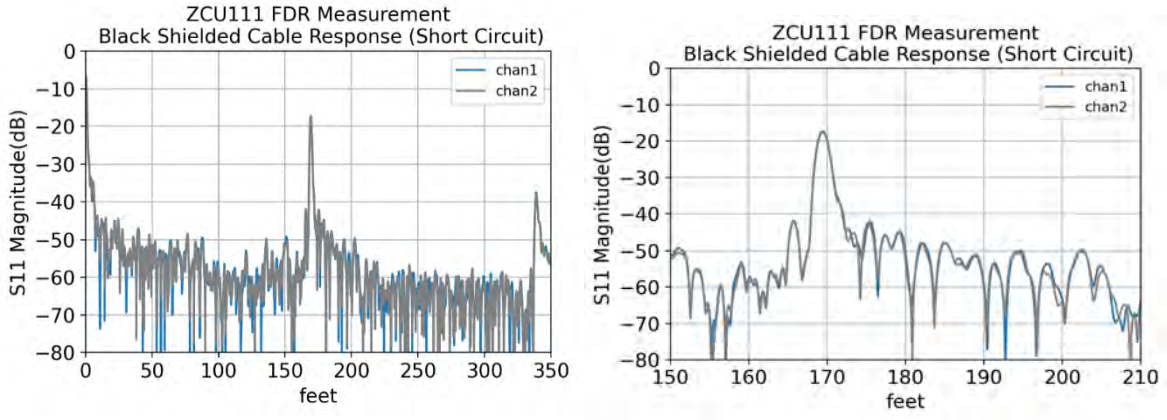

Figure 15. FDR measurement results between channel 1 and 2 for an approximately 170 ft cable.

The utilization of both channels in addition to the possibility of monitoring multiple cables was evaluated by monitoring multiple individual conductors in the low voltage, 170 ft cable simultaneously. In this case the red conductor was shared between channels 1 and 2 with a short jumper cable, and the previously unused black jacketed conductor was now connected to the positive port of channel 2. Figure 16 shows the test configuration breakout at the RF SoC system.

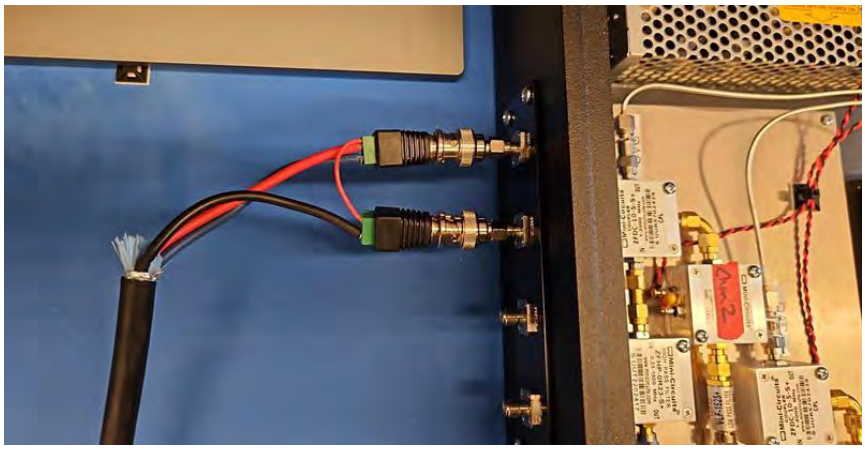

Figure 16. Test configuration for simultaneous multi-conductor monitoring.

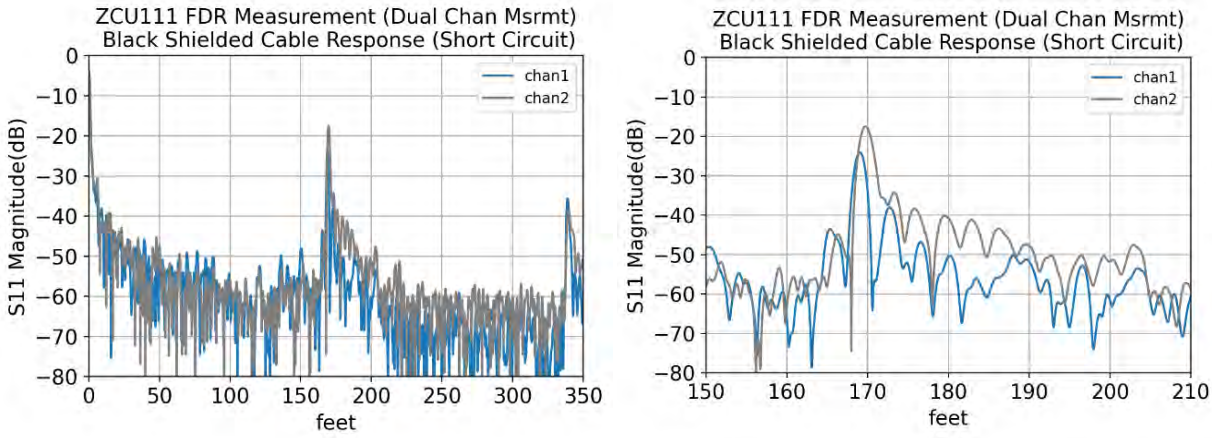

Figure 17. Simultaneous dual channel multi-conductor monitoring FDR responses.

It is evident that there are isolation effects to consider when sharing external conductors between the RF channels. However, even with coupling effects the results show the ability to monitor conductor-to-conductor relationships simultaneously (Figure 17). Further improvements could be made by loading the RF outputs to attenuate externally coupled signals, and frequency domain multiplexing waveforms transmitted from channel 1 to channel 2.

6. LOW VOLTAGE ENERGIZED CABLE TESTING

As a final test for the RF SoC system, measurements were performed on a 200 ft low voltage cable with a defect at 40 ft that was energized to 480 VAC. The Copper Mountain VNA and RF SoC system were connected to the same test configuration, each using the RF current probe to couple onto the cable under test without being directly connected to the 480 VAC (Figure 18). The cable used as a lead from the measurement systems to the coupler was a 20 ft RG58 cable. The test configuration is shown below for the 480 VAC circuit and coupling of the RF measurement systems onto the black jacketed conductor. The fault at 40 ft in on the CUT has the jacket removed for a portion of each of the conductors (Figure 19), a rather gross impedance mismatch effect.

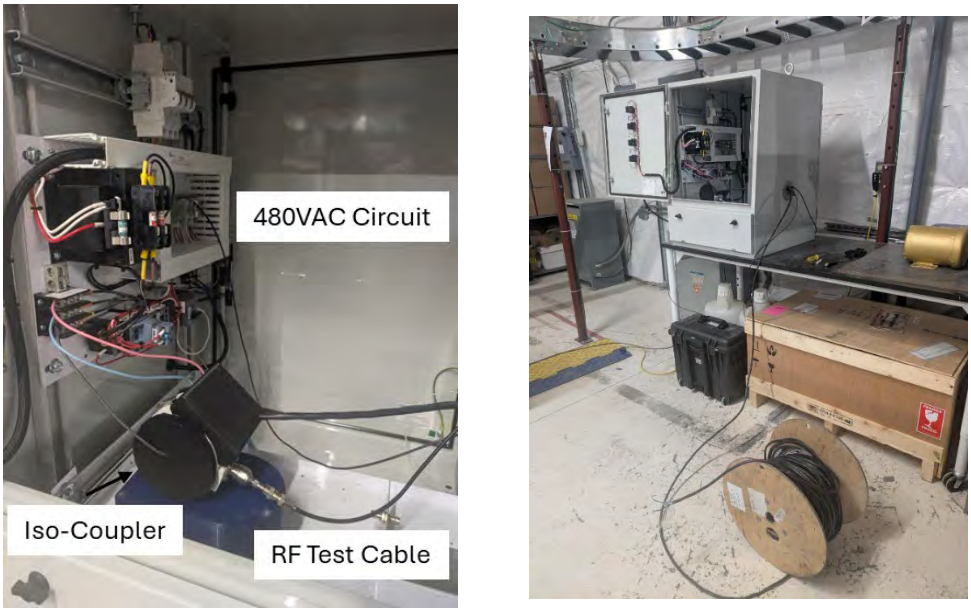

Figure 18. Energized test configuration for RF SoC and VNA FDR.

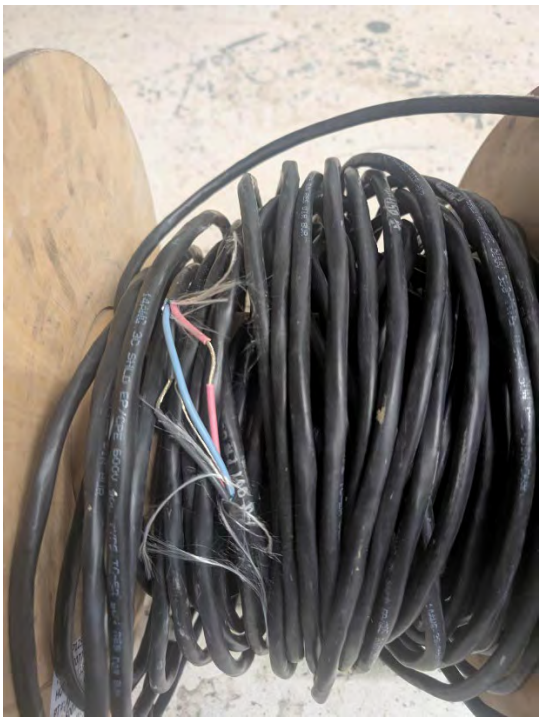

Figure 19. Cable Fault.

The results produced by the Copper Mountain VNA and the RF SoC were similar in magnitude for the injection point registered at 20 ft, the defect at 60ft (40 ft + 20 ft), the two times reflection from the defect, and the end of the cable (Figure 20). Post 100 ft there is an observable difference in the "noise floor" between the two systems. This is assumed to be from calibration accuracy differences between the RF SoC and the Copper Mountain VNA, where subtle errors on the order of 0.01% (-40 dB), begin to set

the dynamic range of measurements. This can be further investigated and potentially improved with slower calibration measurements for reduced noise, also referred to commonly as intermediate-frequency (IF) bandwidth in VNAs.

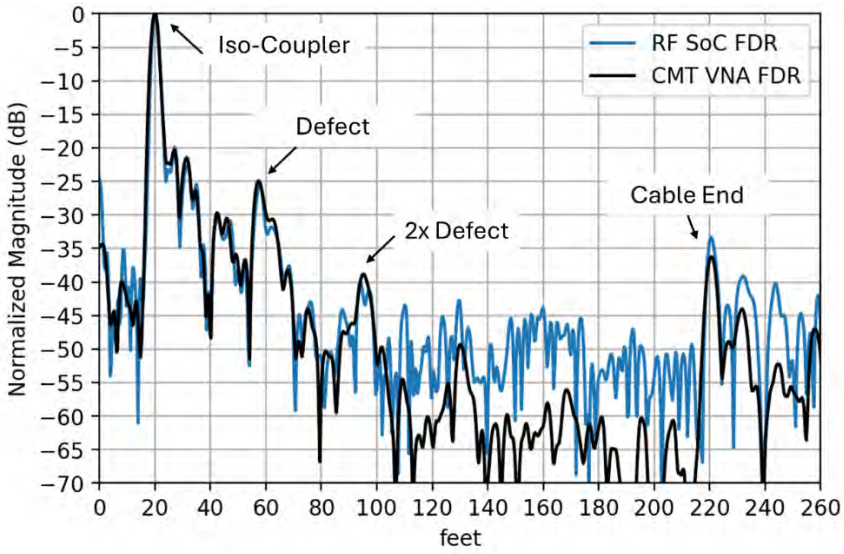

Figure 20. 480 VAC energized 200 ft low voltage cable FDR results for a Copper Mountain VNA vs. the RF SoC system.

7. CONCLUSIONS

This report highlights the performance of the PNNL multi-channel RF SoC reflectometry system through demonstration of its ability to perform both FDR and SSTDR for offline and online testing to detect and locate cable defects. The initial developments of the system enable the FPGA to simultaneously transmit and receive cable test signals on multiple RF channels. The demonstration unit showed two active channels, but the hardware supports expansion up to seven with future PCB development and integration efforts. The measured performance of the RF SoC system compares well to current laboratory grade instrumentation and could serve as the basis for a commercial multi-channel cable monitoring system.

REFERENCES

A.H. Systems. 2023. "Injection Current Probe ICP-622." https://www.ahsystems.com/catalog/ICP-622.php.

Ahmed, N. H., and N. N. Srinivas. 1998. "On-line partial discharge detection in cables." *IEEE Transactions on Dielectrics and Electrical Insulation* 5 (2):181-188. doi: https://doi.org/10.1109/94.671927.

Copper Mountain. 2020. "TR1300/1 2-Port 1.3 GHz Analyzer." accessed 08/29/2022. https://coppermountaintech.com/vna/tr1300-1-2-port-1-3-ghz-analyzer/.

Fluke. 2022. "FLUKE Digital Clamp Meter: Clamp-Jaw Jaw, CAT III 600V/CAT IV 300V, TRMS." accessed 03/15/24. https://www.grainger.com/product/FLUKE-Digital-Clamp-Meter-Clamp-20E891?opr=PLADS&analytics=FM%3APLA&a2c_sku_original=20E890.

Furse C., Y. C. Chung, C. Lo, and P. Pendayla. 2006. "A Critical Comparason Reflectometry Methods for Location of Wireing Faults." *Smart Structures and Systems* 2: 25-46. https://my.ece.utah.edu/~cfurse/Publications/A%20Critical%20Comparison.pdf

Glass, S. W., A. M. Jones, L. S. Fifield, T. S. Hartman, and N. Bowler. 2017. *Physics-Based Modeling of Cable Insulation Conditions for Frequency Domain Reflectometry (FDR).* Pacific Northwest National Laboratory PNNL-26493. Richland, Washington. https://www.pnnl.gov/main/publications/external/technical_reports/PNNL-26493.pdf.

Glass, S. W., J. R. Tedeschi, M. Elen, M. P. Spencer, J. Son, and L. S. Fifield. 2025. "Clamshell Inductive Current Coupler for Online Cable Condition Monitoring." *IEEE Open Journal of Instrumentation and Measurement* 4: 1-8. https://doi.org/10.1109/OJIM.2024.3517623.

Glass, S.W., L.S. Fifield, and Nicola Bowler. 2020. *Cable Nondestructive Examination Online Monitoring for Nuclear Power Plants.* Pacific Northwest National Laboratory PNNL 155612. Richland Washington. https://lwrs.inl.gov/content/uploads/11/2024/03/Cable_NDE_Online_Monitoring.pdf.

Glass, S.W., J R Tedeschi, M.P.; Spencer, J. Son, M. Elen, and L.S. Fifield. 2023. *Laboratory Instrument Software Controlled Spread Spectrum Time Domain Reflectometry for Electrical Cable Testing.* Pacific Northwest National Laboratory PNNL-34511. Richland, Washington. https://doi.org/10.2172/1995282.

Glass, S.W., J. Tedeschi, M.P. Spencer, J. Son, D. Li, M. Elen, and L. S. Fifield. 2023. *Extended Bandwidth Spread Spectrum Time Domain Reflectometry Cable Test for Thermal Aging, Low Resistance Fault, and Water Detection.* Pacific Northwest National Laboratory PNNL-34815. Richland, Washington. https://www.pnnl.gov/main/publications/external/technical_reports/PNNL-34815.pdf.

Glass, S.W., J.R. Tedeschi, M.P. Spencer, J. Son, M.F.N. Taufique, D. Li, M. Elen, L.S. Fifield, J.A. Farber, and A. Al Rashdan. 2024. "Spread Spectrum Time Domain Reflectometry (SSTDR) and Frequency Domain Reflectometry (FDR) Cable Inspection Using Machine Learning." In *Proceedings of the 2024 51st Annual Review of Progress in Quantitative Nondestructive Evaluation*. ASME, Denver, Colorado, July 21–24, 2024. https://doi.org/10.1115/QNDE2024-133645.

Han, J., Y. Zhou, C. Yang, W. Zheng, X. Lu, Y. Wang, J. Han, and L. Geng. 2023. "Review of Research on Running Condition Monitoring of High Voltage Cables." In *2023 IEEE 3rd International Conference on Power, Electronics and Computer Applications (ICPECA)*. IEEE ICPECA, Shenyang, China, January 29-31, 2023. https://doi.org/10.1109/ICPECA56706.2023.10075700.

IEEE. 2015. *IEEE Standard for Qualifying Electric Cables and Splices for Nuclear Facilities*. IEEE Standards Association IEEE 383-2015. Piscataway, NJ. https://doi.org/10.1109/IEEESTD.2015.7287711.

NRC. 2010. *Essential Elements of an Electric Cable Condition Monitoring Program.* Nuclear Regulatory Commission NUREG/CR7000, BNL-NUREG-90318-2009. Washington, D.C. https://www.nrc.gov/reading-rm/doc-collections/nuregs/contract/cr7000/index.

Pyy, Pekka. 2001. "An analysis of maintenance failures at a nuclear power plant." *Reliability Engineering & System Safety*. 72 (3): 293-302. https://doi.org/10.1016/S0951-8320(01)00026-6.
Wirescan. 2022. "LIRALIVE." WireScan. https://www.wirescan.no/wirescan-products.
Yao, L., W. Ma, and C. Yu. 2014. "Correlation between transfer impedance and insertion loss of current probes." *IEEE Electromagnetic Compatibility Magazine* 3: 51-55. https://doi.org/10.1109/MEMC.2014.6849544.

APPENDIX 1: FPGA SOFTWARE

This work was developed under sponsorship from the Department of Energy Light Water Reactor Sustainability program. Software can be made available upon request by contacting the following:

Email: commercialization@pnnl.gov; please reference "IPID 33522-E".